

Second Harmonic Generation of Near-Infrared Semiconductor Laser with Temperature-Dependent Power Control

Banan A. Mefleh

Department of Physics, College of Education, University of Shatra, Shatra, IRAQ

Abstract

In this work, a semiconductor laser of 810nm wavelength and a nonlinear crystalline structure were used to achieve the second harmonic generation. Adjusting the distance between laser diode and a diffraction grating in order to control the output of laser can extend the laser cavity. The parameters such as grating tilt angle, nonlinear medium tilt angle, its temperature, polarization angle and fundamental power and their effects on the second harmonic generation were determined to study the nonlinear generation process. The maximum power of the second harmonic obtained in this work was 112 nW in the violet region.

Keywords: Magnetic sensor; Nickel ferrite; Nanostructures; Plasma sputtering

Received: 17 January 2024; **Revised:** 12 March 2024; **Accepted:** 19 March 2024; **Published:** 1 April 2024

1. Introduction

It might be real to say that no laser has taken large area of interest and technological research in the last two decades as semiconductor lasers did. Many optical and optoelectronic systems make use of these compact lasers for too many applications, such as bar-code scanners and optical data storage. These lasers also have an effective area in spectroscopy and molecular transitions [1-6].

However, free-running commercial semiconductor lasers are not recommended in high-precision spectroscopy since their spectral characteristics do not meet requirements of such field of research [7,8]. Therefore, it is difficult to study the atomic and molecular spectral transitions practically using these lasers neither tune smoothly around same region. However, high-quality wavelength-tunable semiconductor lasers with narrow linewidth could be obtained and used [9-11]. Usually, semiconductor lasers have linewidth of 50 MHz for near infrared (NIR) wavelengths and 7 MHz for visible wavelengths.

The main parameter determining wavelength of semiconductor lasers is the band-gap of the semiconductor itself [12]. Laser wavelength has some dependence on

semiconductor temperature and current density of the diode [13-15]. Effect of temperature appears primarily in the optical path length of laser cavity and gain characteristics of semiconductor [16-18]. Diode current affects diode temperature and carrier density, hence changes refractive index and output wavelength [19-21]. Typically, the behavior of wavelength with temperature is discontinuous due to transferring from a longitudinal mode to another in the cavity [22]. This problem is serious enough to exclude semiconductor lasers from the high-precision spectroscopic studies [23-25].

The limitation of SHG intensity by the coherence length can be overcome by phase matching process employing birefringent crystals [26-28]. This matching process can be satisfied either by varying the angular direction of crystal or its position [29-32]. There are two other nonlinear phenomenon can be achieved using the birefringent crystals. They are frequency mixing and parametric oscillation [33].

The first attempt of second harmonic generation was carried out in 1961 with a ruby laser beam (694 nm) using a quartz crystal. The wavelength conversion efficiency of this attempt was about (10^{-8}) to

the 347 nm wavelength [34]. Nonlinear optics had been appeared as a result of the invention of high intensity lasers. Accordingly, second harmonic generation is now an excellent method to convert wavelengths those not had been obtained from laser transitions known. Also, such phenomenon admits to study and develop nonlinear optics more [35].

2. Experimental Part

The laser system used in this work contains two parts; semiconductor laser and diffraction grating. A 810nm commercial semiconductor laser was used in order to simplify the alignment of laser and mount, then collimating of laser system. The position of collimating lens could be adjusted easily by an adjusting screw. The diffraction grating manufactured by Optometrics (UK) was mounted inside a cylindrical holder with a certain angle. At 810 nm wavelength of semiconductor laser used, the Littrow angle is being 22.5° and the reflectivity into the first order is about 20%.

Figure (1) indicates the experimental set-up of this work. The laser beam is focused onto a 4 cm-long square crystalline sample of gallium selenide (GaSe). The GaSe sample can be tuned by angle and temperature in order to achieve phase matching which is in turn required for efficient second harmonic generation.

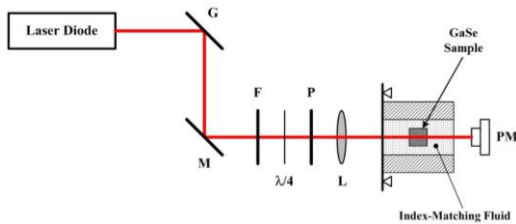


Fig. (1) The experimental set-up of this work

3. Results and Discussion

The conversion efficiency can be greatly enhanced by resonant excitation inside an optical cavity, which increases the average optical intensity. This can also be done by using pulsed instead of CW excitation, which increase the peak intensity. However, none of them will be tried here.

The output power of the second harmonic ($P_{2\omega}$) can be calculated approximately as a function to the incident power (P_{ω}) as [29]:

$$P_{2\omega} = AP_{\omega}^2 \cdot \frac{\sin^2 \Omega}{\Omega^2} \tag{1}$$

where A is a constant depending on geometry and crystal, $\Omega = \frac{l \cdot \Delta k}{2}$, l is length of the nonlinear crystal, Δk is the phase mismatch between the two waves, and the term $\sin^2 \Omega / \Omega^2$ represents the conversion efficiency per unit length

This formula is valid if the depletion of the fundamental beam is being neglected and a plane wave is being used. Figure (2) shows the power of second harmonic as a function to the fundamental power. Experimentally, some deviation of about 1% from the results of the formula above would be observed due to the divergence property of the focused laser beam [36].

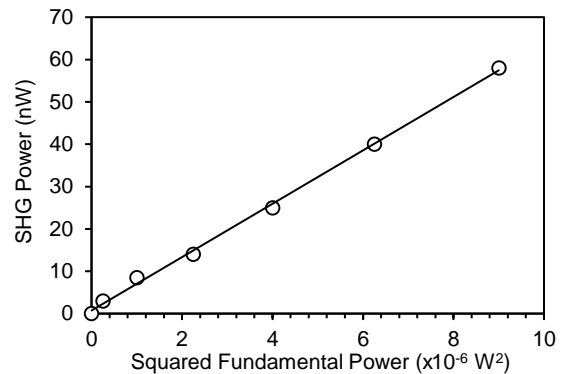


Fig. (2) The power of second harmonic as a function to the fundamental power

The laser can be tuned by adjusting angle and distance between the laser and diffraction grating. The set-up described here for mirror mount can provide tuning of 5 nm. In order to reflect larger fraction of light back into the laser cavity, the grating must be selected to achieve such function. Figure (3) shows the tuning range at 810 nm as a function to grating angle.

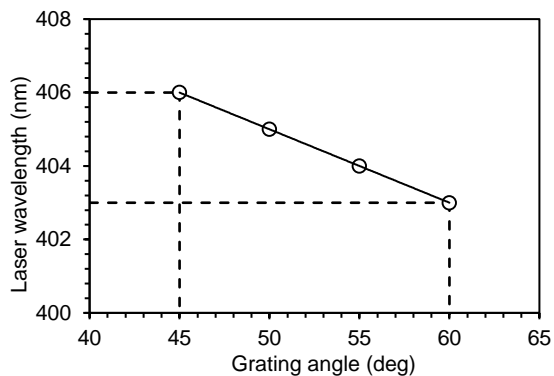


Fig. (3) The tuning range at 403 nm as a function to grating angle

It is well known that the light incident on a nonlinear medium at a frequency (ω) and the light generated due to nonlinear effect at frequency (2ω) pass the medium with different speeds. Hence, they are not necessarily in phase within the nonlinear crystal and an interference effect results within the crystal. The second harmonic generation is then inefficient [29,37]. In order to eliminate the interference effect, the dispersion of the crystal material with the temperature as well as polarization dependence of the refractive index is being offset. Due to propagation direction through the crystal, the refractive index and velocity of the extraordinary wave are varied. Thus the refractive index of the crystal to the ordinary wave of frequency (ω) is half of that extraordinary [29].

Most materials that are transparent in the visible have a refractive index that decreases with increasing wavelength and the corresponding wavevector mismatch is lower than zero. Therefore, it is impossible to achieve efficient second harmonic generation in these materials unless a way is found to phase-match the interaction. In this work, angle tuning of birefringent crystal is a used to modify the refractive indices and tune the phase matching.

In order to vary the temperature of crystal, it is immersed in a fluid characterized as an "index-matching" in a thermal jacket with a simple heater. Figure (4) represents the relation of second harmonic power to the crystal temperature. The output beam is filtered to prevent the

fundamental laser light and permit the second harmonic generated (frequency-doubled) light to transmit. The latter is in the violet region (403-406 nm) of visible range as the fundamental is red (806-812 nm). A photomultiplier tube is used as a detector and connected to a micrometer.

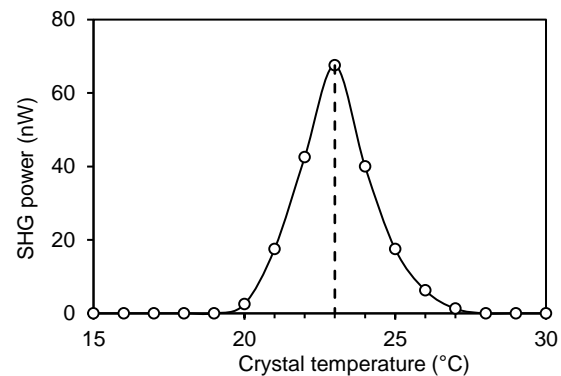


Fig. (4) The relation of second harmonic power to the crystal temperature

4. Conclusions

Regarding to results obtained in this work, the second harmonic generation with 810 nm semiconductor laser and a GaSe crystalline sample was achieved. The nonlinear effect in the GaSe crystalline medium resulting the second harmonic generation was studied and introduced with respect to some parameters to be so active on such process. These parameters are grating angle, GaSe sample angle, its temperature, polarization angle and fundamental power. The maximum second harmonic power obtained at the optimum conditions was (112 nW) in the ultraviolet region (403-406 nm).

References

- [1] A. Comby, D. Descamps, S. Beauvarlet, A. Gonzalez, F. Guichard, S. Petit, Y. Zaouter and Y. Mairesse, *Opt. Exp.*, 27(15) (2019) 20383-20396.
- [2] Z.-J. Yang, Q. Zhao, Y.-H. Deng, D. Zhang and J. He, *Opt. Exp.*, 26(5) (2018) 5835-5844.
- [3] A. Villosio and D.V. Skryabin, *Opt. Exp.*, 27(5) (2019) 7098-7107.
- [4] Y. Liu, S.L. Liang, G.R. Jin and Y.B. Yu, *Opt. Exp.*, 28(3) (2020) 2722-2731.
- [5] B. Lu and D.H. Torchinsky, *Opt. Exp.*, 26(25) (2018) 33192-33204.
- [6] C. Eigner, M. Santandrea, L. Padberg, M.F. Volk, C.E. Rüter, H. Herrmann, D. Kip and C.

- Silberhorn, *Opt. Exp.*, 26(22) (2018) 28827-28833.
- [7] C. Yuan, Z. Wang, T.K. Borg, T. Ye, C. Baicu, A. Bradshaw, M. Zile, R.B. Runyan, Y. Shao and B.Z. Gao, *Biomed. Opt. Exp.*, 10(7) (2019) 3183-3195.
- [8] C.B. Marble, S.P. O'Connor, D.T. Nodurft, A.W. Wharmby and V.V. Yakovlev, *Opt. Exp.*, 27(3) (2019) 2828-2836.
- [9] C.-H. Yeh, C.-Z. Tan, C.-H.A. Cheng, J. Hung and S.-Y. Chen, *Biomed. Opt. Exp.*, 9(12) (2018) 6081-6090.
- [10] E. Nitiss, O. Yakar, A. Stroganov and C.-S. Bres, *Opt. Lett.*, 45(7) (2020) 1958-1961.
- [11] G. Orenstein, A. Julie Uzan, S. Gadasi, T. Arusi-Parpar, M. Krüger, R. Cireasa, B.D. Bruner and N. Dudovich, *Opt. Exp.*, 27(26) (2019) 37835-37845.
- [12] H. Conradi, A. Hakmi, M. Kleinert, L. Liebermeister, D. de Felipe, M. Weigel, M. Kresse, C. Zawadzki, B. Globisch, N. Keil, R. Freund and M. Schell, *J. Lightwave Technol.*, 39(7) (2021) 2123-2129.
- [13] H.-C. Tai, P.-L. Chen, J.-W. Xu and S.-Y. Chen, *Opt. Exp.*, 28(26) (2020) 38831-38841.
- [14] I.J. Hong, K. Lee and J.H. Lee, *Opt. Exp.*, 28(17) (2020) 25431-25443.
- [15] J. Defrance, M. Schäferling and T. Weiss, *Opt. Exp.*, 26(11) (2018) 13746-13758.
- [16] J. Xu, E. Plum and V. Savinov, *Opt. Exp.*, 28(22) (2020) 33346-33354.
- [17] J. Yeo, Q. Ran, A. Tan and H. Li, *Opt. Exp.*, 28(19) (2020) 28164-28177.
- [18] L. Carletti, D. de Ceglia, M.A. Vincenti and C. de Angelis, *Opt. Exp.*, 27(22) (2019) 32480-32489.
- [19] L. Rodriguez-Sune, J. Trull, C. Cojocar, N. Akozbek, D. de Ceglia, M.A. Vincenti and M. Scalora, *Opt. Exp.*, 29(6) (2021) 8581-8591.
- [20] L. Rodríguez-Suné, J. Trull, M. Scalora, R. Vilaseca and C. Cojocar, *Opt. Exp.*, 27(18) (2019) 26120-26130.
- [21] M. Li, C.-L. Zou, C.-H. Dong and D.-X. Dai, *Opt. Exp.*, 26(21) (2018) 27294-27304.
- [22] M. Santandrea, M. Stefszky, G. Roeland and C. Silberhorn, *Opt. Exp.*, 28(4) (2020) 5507-5518.
- [23] M. Stefszky, M. Santandrea, F. vom Bruch, S. Krapick, C. Eigner, R. Ricken, V. Quiring, H. Herrmann and C. Silberhorn, *Opt. Exp.*, 29(2) (2021) 1991-2002.
- [24] M.H. Shor Peled, E. Toledo, S. Shital, A. Maity, M. Pal, Y. Sivan, M. Schwartzman and A. Niv, *Opt. Exp.*, 28(21) (2020) 31468-31479.
- [25] P. Xia, C. Kim, F. Lu, T. Kanai, H. Akiyama, J. Itatani and N. Ishii, *Opt. Exp.*, 26(22) (2018) 29393-29400.
- [26] R. Jafari, T. Jones and R. Trebino, *Opt. Exp.*, 27(3) (2019) 2113-2124.
- [27] S. Chakraborty, S.-T. Chen, Y.-T. Hsiao, M.-J. Chiu and C.-K. Sun, *Biomed. Opt. Exp.*, 11(2) (2020) 571-585.
- [28] S. Liu, K. Switkowski, X. Chen, T. Xu, W. Krolikowski and Y. Sheng, *Opt. Exp.*, 26(7) (2018) 8628-8633.
- [29] Yariv, A., 1997, "**Optical Electronics in Modern Communications**", 5th Edition, Saunders College Publishing (Oxford), pp.285-299.
- [30] S.-L. Lee, Y.F. Chen and C.-Y. Dong, *Biomed. Opt. Exp.*, 10(10) (2019) 5223-5234.
- [31] Svelto, O., "**Principles of Lasers**", Plenum Press (New York), 1998, Ch.8.
- [32] S.W. Hancock, S. Zahedpour and H.M. Milchberg, *Optica*, 8(5) (2021) 594-597.
- [33] T. Ning, X. Li, Z. Zhang, Y. Huo, Q. Yue, L. Zhao and Y. Gao, *Opt. Exp.*, 29(11) (2021) 17286-17294.
- [34] T.V. Murzina, V.V. Radovskaya, I.Y. Pashen'kin, N.S. Gusev, A.I. Maydykovskiy and E.A. Mamonov, *Opt. Exp.*, 29(2) (2021) 2106-2111.
- [35] W. Wang, B. Wu, S. Lin, X. Li, J. Liu and J. Tan, *Opt. Exp.*, 27(14) (2019) 19737-19748.
- [36] X. Xue, X. Zheng and B. Zhou, *Phot. Res.*, 6(10) (2018) 948-953.
- [37] Pedrotti, F. L. and Pedrotti, L. S., 1987, "**Introduction to optics**", 2nd Edition, Prentice-Hall (New Jersey), p. 543.
- [38] Koechner, W., 1992, "**Solid-State Laser Engineering**", 3rd Edition, Springer-Verlag (New York), pp. 485.
- [39] Y. Gao and B. Ge, *Opt. Exp.*, 29(5) (2021) 6903-6914.
- [40] D.N. Nikogosyan, 2005, "**Nonlinear Optical Crystals: A Complete Survey**", Springer Science+Business Media, Inc. (New York), pp. 108-112.
- [41] M. Isik, E. Tugay and N.M. Gasanly, *Philos. Mag.*, 96(24) (2016) 2564-2573.
- [42] A. Chandra Das, S. Bhattacharya, M. Jewariya, S.S. Prabhu, K.C. Mandal, T. Ozaki and P. Kumar Datta, *IEEE J. Sel. Top. Quantum Electron.*, 23(4) (2017) 8400607.